Efficiency Analysis for Deep Brain Stimulation Using an LCC-C WPT System Operating at 13.56 MHz Frequency

Kemal ŞAHİN[1], Sevilay ÇETİN[2]

[1]Department of Biomedical Engineering, Pamukkale University, Denizli, Turkey ksahin161@posta.pau.edu.tr
[2]Department of Biomedical Engineering, Pamukkale University, Denizli, Turkey scetin@pau.edu.tr

Abstract

This study aims to meet the power demand of a near field implant in a fixed location for DBS (Deep Brain Stimulation) devices. In this context, a WPT (Wireless Power Transfer) system using LCC-C compensation is proposed. With LCC-C topology, the battery of the DBS device can be efficiently charged at low power levels. The operation frequency is set as 13.56 MHz, which is high enough and within the ISM (Industrial Scientific and Medical) band standards. For the LCC-C topology, electrical performance analysis in simulation environment has been discussed. Based on simulation results, the DC output voltage of 2.57 V is successfully regulated in the case of optimal alignment at a distance of 5 mm. In the simulated tissue environment, the proposed topology exhibits a PTE (Power Transfer Efficiency) of 12.73%. Efficiency analyses in case of misalignment, which are among the possible conditions, are also presented.

1. Introduction

In addressing neurological disorders like Parkinson's ailment, essential tremor, and epilepsy, implantable DBS (Deep Brain Stimulation) devices can be used as an effective solution where drugs and other treatment modalities fall short [1]. DBS devices can provide fewer side effects and higher efficiency compared to drugs [1]. DBS devices have shown positive, stable and safe results in the long term treatments [2].

Traditional implantable DBS devices have limited battery capacity [3]. Depending on the frequency of use, they need to be replaced at certain intervals. This need for replacement in traditional batteries also brings infection risks and cost disadvantages as it requires surgical intervention [2]–[4].

Traditional DBS batteries are placed in the chest area [5]. This placement creates a disadvantage in terms of patient and operation time since it requires a two stage surgical operation [5]. Thus, the large battery and long cables negatively affect patient comfort.

Thanks to WPT (Wireless Power Transfer) technologies, rechargeable batteries with smaller size and capacity can be used. Thus, head mounted DBS systems, which is not required surgical operation with anesthesia, can be implemented for the patients. Recently, head mounted DBS systems have been studied in the literature [6], [7].

Based on these studies, the ability to charge miniaturized DBS systems that can be implanted in the head region with WPT provides a number of advantages such as potential adverse effects of anesthesia, eliminating the risk of infection during the replacement of traditional DBS batteries, eliminating aesthetic concerns due to battery size, eliminating the discomfort caused by cables passing over the neck.

WPT systems have gained popularity due to the advantages of rechargeability of implantable devices. Many studies have focused on the development or utilization of WPT systems in the field of DBS [6]–[8].

WPT is created using coils with weak coupling, the use of compensation circuit is important to achieve higher efficiency [9]. In inductive coupling, power transmission can be enhanced by a resonant capacitor. Magnetic resonant coupling topologies can be basically classified into four groups: Series-Serial, Series-Parallel, Parallel-Serial and Parallel-Parallel [3].

In addition to basic topologies, there are also hybrid topologies developed in the literature. Hybrid topologies such as LCC-C have the potential to eliminate the disadvantages faced by conventional topologies [10]. At the same time, they can stand out with their advantages such as voltage regulation capability and freedom of control [11]. In [12], LCC-C topology is compared with SS topology. The system is compared by changing the load resistance under ideal conditions. In this comparison, the ability of the SS topology to provide constant current and the tendency of the LCC-C topology to provide constant voltage are observed and it is concluded that the LCC-C configuration is more favorable for low power transfer.

Given the limited space requirement of implanted DBS devices, the LCC-C topology has the advantage of having only a series connected capacitor at the receiver side. This topology has been used as a preferred option for near field implantation [6]

The 13.56 MHz frequency is situated within the ISM (Industrial, Scientific, and Medical) frequency band, has been selected as the operating frequency, and this frequency has been frequently used in implantable WPT systems [7], [13].

Some studies in the literature on WPT systems operating at 13.56 MHz frequency developed for implantable devices were examined. In similar study, WPT implants placed in the head region at a frequency of 13.56 MHz utilized LCC-C topology for efficient power transfer over a distance of 10 mm within the tissue [6]. In [6] and [7], complex designs with three and four coils for efficient power transfer in weak coupling are proposed. In this study, a simpler WPT system using only two coupling coils is proposed. As a placement location, it is proposed to be placed on the parietal bone at a distance of 5 mm in a soft tissue environment.

The 3D design and magnetic analysis of the coupling coils were carried out using ANSYS software. Subsequently, electric-magnetic common simulation has been carried out to test Power Transfer Efficiency (PTE) performance of the proposed WPT system.

2. Proposed WPT System Design

As an alternative to conventional DBS devices, the concept design shown in Fig. 1 is proposed. Fig. 1 (a) shows the layout of the proposed DBS circuit on the head. Fig. 1 (b) shows the LCC-C compensation circuit. This design involves an arrangement in which the receiving implant coil is placed on the parietal bone tissue in an adipose tissue environment. Detailed modeling of the tissues is shown in Fig. 2 In the design, using the WPT technique, the power induced on the receiver coil is transmitted through short cables to a stimulation module called IPG (Implanted Pulse Generator). The IPG module includes basic modules such as battery, power control, communication and stimulation. The design includes an arrangement in which the IPG is positioned at some distance from the coil to minimize magnetic interference from the metal parts of the IPG module and to maintain the thinness of the IPG module. This will provide a more advantageous positioning compared to through the neck systems.

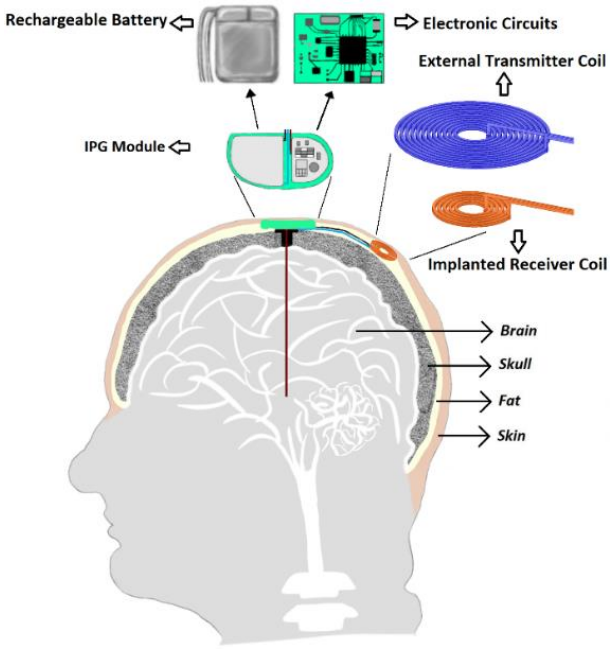

(a)

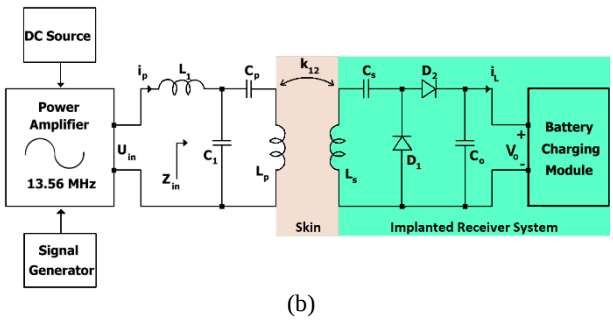

(b)

Fig. 1. WPT system (a) Configuration of the proposed conceptual WPT system for DBS and (b) LCC-C topology

The IPG module basically consists of two parts. First, a small rechargeable battery, which stores the wirelessly transmitted energy to keep the IPG running continuously. Second, miniaturized electronic circuits to fulfill the stimulation function of the IPG. In this work, we focus on the design of an efficient WPT utilizing the characteristics of constant output voltage at low power levels. The Power Amplifier (PA) generates a sinusoidal voltage at 13.56 MHz, which is then applied to the LCC-C compensation circuit depicted in Fig 1 (b). The input voltage is indicated as U_{in} and the input impedance as Z_{in}. L_P is the transmitter coil and L_S is the receiver coil. These two coils are connected with a weak coupling coefficient k_{12}. On the transmitter, the LCC compensation network consisting of L_1, C_1, C_P. On the receiving side, the compensation capacitor Cs is connected in series with the coil Ls. The induced AC voltage is rectified by diodes D_1 and D_2. In the system used, the simultaneous use of a diode rectifier and a voltage doubler circuit provides a boost regulation effect rectifier output. The out voltage Vo, filtered by the capacitor Co, is transmitted to the battery charging module, which is assumed as the load.

2.1. Design of Coupling Coils

Especially for implantable devices, efficiency is important at high frequency and low power levels in a limited space. In order to ensure targeted efficiency, the quality factor, the coupling factor, the coil wire parameters should be taken into consideration. Quality factor (Q) can be written as follows:

$$Q = \frac{\omega L_{Coil}}{R_{Coil}}. \tag{1}$$

Where ω is the angular frequency, R_{Coil} is the resistance of a coil, L_{Coil} is the inductance value of a coil.

The coupling coefficient (k) factor indicates how effective the magnetism between the coupling coils and it can be written as

$$k = \frac{M}{\sqrt{L_P L_S}}. \tag{2}$$

The coupling factor varies in the range $0 \leq k < 1$. Here M is the mutual inductance between the coupling coils. L_P, L_S are the inductances of the transmitting and receiving coils, respectively.

Skin effect (δ) is also important parameter to reduce conduction losses of the coupling coils, especially at high frequencies. The skin effect can be written as

$$\delta = \sqrt{\frac{\rho}{\pi f \mu}}. \tag{3}$$

In this context, δ represents the depth of immersion, μ represents the magnetic permeability of the conductor, ρ stands for the resistivity of the material, and f represents the operating frequency. Due to space constraints, the receiver coil is designed in a small size of 5 mm in diameter. A design with two coils built on the FR4 board is presented. Inductance values, coupling between coils and internal resistances of the coils were extracted by ANSYS simulation.

In implantable WPT studies, the power transfer distance was realized at different distances depending on the depth of the implant [6], [14]. In this study, skin, brain, fat layer and parietal bone tissue layers were considered. The thickness of these tissues can vary from person to person [13], [15], [16]. Biological tissues were modeled on a tissue basis according to the data given in ANSYS software [17].

The position of the receiving coil is planned to be above the bone tissue. The power transfer distance between the coils was determined as 5 mm. Fig. 2 illustrates the cross-sectional positioning of the modeled tissues.

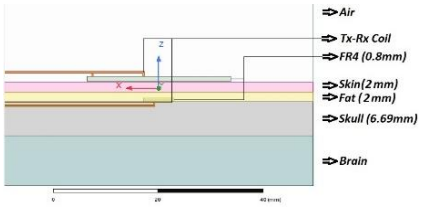

Fig. 2. The cross-sectional view of modeled tissues on ANSYS software.

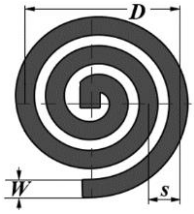

Fig. 3. Coil scaling parameters

Fig. 3 shows the scaling parameters of the transmit and receive coils. Simulation and design parameters are Table 1 shows. Here, N represents the number of windings, and t denotes the thickness of the PCB path.

Table 1. Simulation and design parameters of the coils

Parameter	L_P	L_S
L(μH)	5.774	0.1308
R(Ω)	1.724	0.193
D(mm)	25.5	5
s	0.5	0.35
N	20	5
W(mm)	0.3	0.2
t(mm)	0.035	0.035

The sliding motion of the coils in the horizontal and vertical axes is simulated for imperfect conditions. In the vertical axis, the coil distance ranged from 5 mm to 10 mm. In the horizontal plane, the misalignment tolerance ranged from 5 mm to 10 mm. The graph showing the coupling change is given in Fig. 4.

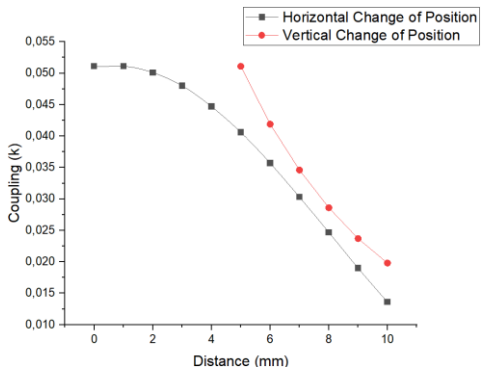

Fig. 4. Coupling variation obtained due to position change in the vertical and horizontal plane

2.2. The LCC-C Compensation Topology Design

The circuit schematic of the WPT circuit with LCC-C topology, is depicted in Fig. 5. On the transmitter side, the an LCC compensation network, comprising L_1, C_1, and C_P elements, is employed to compensate for reactive power. At the receiver side, L_S coil is serially connected with the C_S capacitor. The circuit model also includes the coil resistances that occur under non ideal conditions; R_{L1}, R_{LP} and R_{LS} are the expressed values. R_{Load} represents the output load. In the analysis, the output load is 50 Ω and R_{L1} resistance is 0.2 Ω. When obtaining the DC voltage, the forward voltage of diodes D_1 and D_2 is assumed to be 0.3 V. U_{ac} represents the voltage across the resistor at the topology output.

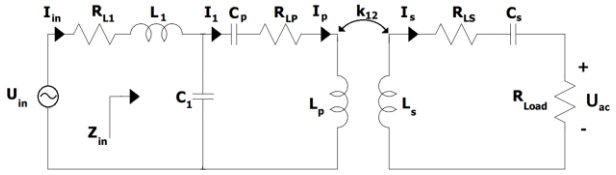

Fig. 5. The LCC-C compensation circuit model

For zero phase angle operation of the circuit, calculations of the circuit parameters are extracted as given in [18].

Based on [18], obtaining the inductance L_1 can be written as

$$L_1 = kU_{in}\sqrt{\frac{L_P L_S}{R_{Load} P_{out}}}. \tag{4}$$

Where P_{out} is the output power of the load. The value of the C_1, C_P and C_S capacitors can be written as

$$C_1 = \frac{1}{L_1\omega^2}. \tag{5}$$

$$C_P = \frac{1}{\omega^2(L_P - L_1)}. \tag{6}$$

$$C_S = \frac{1}{\omega^2 L_S}. \tag{7}$$

The PTE (η) of the WPT system for DBS is expressed as follows:

$$\eta = \frac{P_{out}}{P_{in}}. \tag{8}$$

Where P_{out}, P_{in} represent the power measured across the load and the input power of the circuit, respectively.

3. Simulation Results

The LCC-C circuit parameters are calculated according to 5 mm are given in Table 2.

Table 2. LCC-C Circuit values

Parameters	Value
L_1	276.05nH
C_1	499.03 pF
C_P	25.056 pF
C_S	1053.21 pF
k	0.051147

The DC current and voltage regulation graphs obtained on the output load depending on the axial distance variation are given in Fig. 6. Fig. 6(a) and Fig. 6(b) show the output voltage and the current variation, respectively. The PTE variation of the WPT topology is given in Fig. 7.

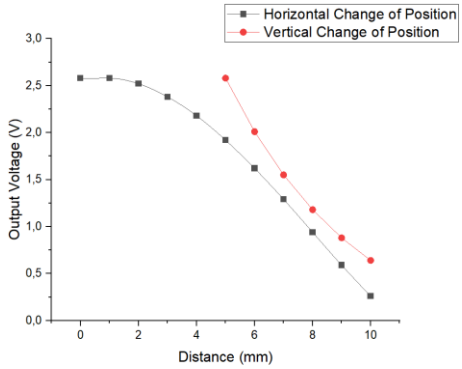

Fig. 6. (a) The output voltage value and (b) current value obtained depending on the position change in the vertical and horizontal planes

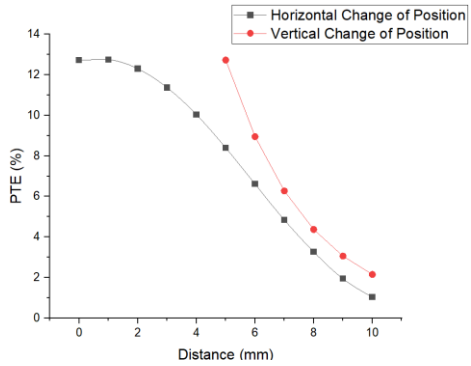

Fig. 7. The PTE variation obtained as a function of position change in the vertical and horizontal planes

4. Conclusions

This paper proposes a WPT system that can facilitate the head mount ability of DBS devices. The design and simulation of the proposed LCC-C topology has been successfully realized and shown to be an effective approach to achieve appropriate electrical outputs. The designed system has a simple structure and consists of two coils.

A near field implanted coil delivered 41.61 mW of power with 12.73% efficiency between perfectly aligned coils at a distance 5 mm. The PTE of the system is achieved as 8.40% at a horizontal misalignment of 5 mm with a coupling coil separation of 5 mm.

At a distance of 5 mm, the simultaneous use of a diode rectifier with a voltage doubler circuit between perfectly aligned coils provides a step-up regulation effect resulting in DC 2.57 V and 51.3 mA at the rectifier output. With the addition of the step-up rectifier structure to the system, the end to end efficiency was measured as 26.06%.

5. Acknowledgement

Pamukkale University provides support for this research under the grant reference 2022FEBE051.

6. References

[1] M. Parastarfeizabadi and A. Z. Kouzani, "Advances in closed-loop deep brain stimulation devices," *J. NeuroEngineering Rehabil.*, vol. 14, no. 1, p. 79, Aug. 2017.

[2] V. Salanova *et al.*, "The SANTÉ study at 10 years of follow-up: Effectiveness, safety, and sudden unexpected death in epilepsy," *Epilepsia*, vol. 62, no. 6, pp. 1306–1317, 2021.

[3] A. I. Mahmood, S. K. Gharghan, M. A. Eldosoky, and A. M. Soliman, "Near-field wireless power transfer used in biomedical implants: A comprehensive review," *IET Power Electron.*, vol. 15, no. 16, pp. 1936–1955, 2022.

[4] Y. Ben Fadhel, S. Ktata, K. Sedraoui, S. Rahmani, and K. Al-Haddad, "A Modified Wireless Power Transfer System for Medical Implants," *Energies*, vol. 12, no. 10, Art. no. 10, Jan. 2019.

[5] C. Sarica *et al.*, "Implantable Pulse Generators for Deep Brain Stimulation: Challenges, Complications, and Strategies for Practicality and Longevity," *Front. Hum. Neurosci.*, vol. 15, 2021.

[6] S. Cetin, V. Yenil, and U. A. Dere, "An Efficient Wireless Power Transfer System for An Implantable Deep Brain Stimulation," in *2022 International Conference on Applied Electronics (AE)*, Sep. 2022, pp. 1–4.

[7] C.-L. Yang, C.-K. Chang, S.-Y. Lee, S.-J. Chang, and L.-Y. Chiou, "Efficient Four-Coil Wireless Power Transfer for Deep Brain Stimulation," *IEEE Trans. Microw. Theory Tech.*, vol. 65, no. 7, pp. 2496–2507, Jul. 2017.

[8] J. Kim, S. Park, S. Oh, Y. Huh, J. Cho, and J. Oh, "Cage-Embedded Crown-Type Dual Coil Wireless Power Transfer Based Microwave Brain Stimulation System for Untethered and Moving Mice," *IEEE Trans. Biomed. Circuits Syst.*, vol. 17, no. 2, pp. 362–374, Apr. 2023.

[9] S. Cetin and Y. E. Demirci, "High-efficiency LC-S compensated wireless power transfer charging converter for implantable pacemakers," *Int. J. Circuit Theory Appl.*, vol. 50, no. 1, pp. 122–134, 2022.

[10] Y. Wang, H. Wang, T. Liang, X. Zhang, D. Xu, and L. Cai, "Analysis and design of an LCC/S compensated resonant converter for inductively coupled power transfer," in *2017 IEEE Transportation Electrification Conference and Expo, Asia-Pacific (ITEC Asia-Pacific)*, Aug. 2017, pp. 1–5.

[11] S. Wang, B. Wei, Q. Bo, C. Xu, and J. Xu, "Analysis of Output Characteristics of LCC-C Inductively Coupled Power Transfer System," in *2019 IEEE 3rd International Electrical and Energy Conference (CIEEC)*, Sep. 2019, pp. 845–850.

[12] Y. Chen, H. Zhang, C.-S. Shin, K.-H. Seo, S.-J. Park, and D.-H. Kim, "A Comparative Study of S-S and LCC-S Compensation Topology of Inductive Power Transfer Systems for EV Chargers," in *2019 IEEE 10th International Symposium on Power Electronics for Distributed Generation Systems (PEDG)*, Jun. 2019, pp. 99–104.

[13] K. Mohanarangam, Y. Palagani, and J. R. Choi, "Evaluation of Specific Absorption Rate in Three-Layered Tissue Model at 13.56 MHz and 40.68 MHz for Inductively Powered Biomedical Implants," *Appl. Sci.*, vol. 9, no. 6, Art. no. 6, Jan. 2019.

[14] T. Campi, S. Cruciani, V. De Santis, F. Maradei, and M. Feliziani, "Near Field Wireless Powering of Deep Medical Implants," *Energies*, vol. 12, no. 14, Art. no. 14, Jan. 2019.

[15] H. J. Choi, R. K. De Silva, D. C. Tong, H. L. De Silva, R. M. Love, and J. Athens, "The Thickness of Parietal Bones in a New Zealand Sample of Cadaveric Skulls in Relation to Calvarial Bone Graft," *Craniomaxillofacial Trauma Reconstr.*, vol. 6, no. 2, pp. 115–120, Jun. 2013.

[16] A. Drossos, V. Santomaa, and N. Kuster, "The dependence of electromagnetic energy absorption upon human head tissue composition in the frequency range of 300-3000 MHz," *IEEE Trans. Microw. Theory Tech.*, vol. 48, no. 11, pp. 1988–1995, Nov. 2000.

[17] "Database Summary » IT'IS Foundation." Accessed: Sep. 26, 2023. [Online]. Available: https://itis.swiss/virtual-population/tissue-properties/database/database-summary/

[18] M. Kim, D.-M. Joo, and B. K. Lee, "Design and Control of Inductive Power Transfer System for Electric Vehicles Considering Wide Variation of Output Voltage and Coupling Coefficient," *IEEE Trans. Power Electron.*, vol. 34, no. 2, pp. 1197–1208, Feb. 2019.